Stem Cell Research (2011) 7, 163–171

available at www.sciencedirect.com

ScienceDirect

www.elsevier.com/locate/scr

SHORT REPORT

Both human and mouse mesenchymal stem cells promote breast cancer metastasis

Stella Maris Albarenque, Ralf Michael Zwacka, Andrea Mohr*

National University of Ireland, Galway, National Centre for Biomedical Engineering Science, Molecular Therapeutics Group, Galway, Ireland

Received 7 July 2010; received in revised form 27 April 2011; accepted 2 May 2011
Available online 10 May 2011

Abstract Cell therapy has the potential to offer novel treatment modalities for a number of diseases including cancer, and stem cells and in particular mesenchymal stem cells (MSCs) have been experimentally used to deliver therapeutic transgenes. However, conflicting reports have on the one side found that human MSCs can promote metastasis, while on the other hand other studies have shown that MSCs can stall the growth of metastatic lesions. In order to clarify the role of MSCs in metastasis development, we tested whether murine MSCs would behave similarly to human cells in mice. We found that the tissue distribution of human and mouse MSCs was nearly identical after intravenous injection. In mice with MDA-MB-231 mammary carcinoma xenografts we found that a fraction of MSCs infiltrated the primary tumor mass, but that the general tissue distribution of MSCs was unaffected by the tumor-burden. About half of the tumor-burdened animals that were treated with murine and human MSCs, respectively, harbored metastatic lesions with only 17% of controls showing metastatic nodules. Hence, both human and mouse MSCs possess metastasis-promoting activity raising concerns about the safe use of MSCs, but at the same time making the use of murine transgenic model systems feasible to study the role of MSCs in metastasis development and possibly finding ways of using them safely as cell therapeutic vehicles.

Introduction

Metastasis is the most frequent and life-threatening complication associated with cancer. It is estimated that more than 90% of deaths in cancer patients are due to the direct or indirect effects of metastasis (Sleeman and Steeg, 2010). Despite of substantial advances in our knowledge regarding tumor treatments, the attempts to cure advanced cancer patients are still hampered by the extent and heterogeneity of the tumor burden, the acquisition of multiple drug resistance and survival mechanisms in the diverse population of cells that comprise advanced metastatic lesions (Sporn, 1996). Thus, novel treatment approaches are urgently needed.

Cell therapy is an emerging medical field that opened the possibility for the treatment of a wide range of pathologies including cancer. In recent years several research groups have reported on the successful use of unaltered or engineered MSCs for the treatment of tumors including metastatic lesions in various model systems (Studeny et al., 2002; Mohr et al., 2010). MSCs are stromal cells that normally reside within the adult bone marrow and are able to differentiate into many adult cell types such as osteocytes, chondrocytes and adipocytes (Barry and Murphy, 2004; Dominici et al., 2006). Recent studies have shown their ability to migrate and home to injured and tumor sites and their utility as anti-tumor cell and gene therapy vehicle is based on these characteristics

* Corresponding author at: National University of Ireland, Galway, National Centre for Biomedical Engineering Science, (NCBES), University Road, Galway, Ireland. Fax: +353 91 49 4596.
E-mail address: andrea.mohr@nuigalway.ie (A. Mohr).

1873-5061/$ - see front matter © 2011 Elsevier B.V. All rights reserved.
doi:10.1016/j.scr.2011.05.002

(Khakoo et al., 2006; Kidd et al., 2009; Zhang et al., 2009; Son et al., 2006; Hall et al., 2007). This means that systemically administered MSCs following transduction with non-viral or viral vectors that contain specific tumoricidal transgenes can seek out sites of malignant growth and deliver their therapeutic payload (Baksh et al., 2004; Motaln et al., 2010). However, the last few years have also witnessed a growing controversy about the effects of MSCs on tumor cells with some publications reporting a metastasis-promoting activity (Karnoub et al., 2007; Molloy et al., 2009), whereas others showed inhibition of tumor cell growth and dissemination by MSCs (Khakoo et al., 2006; Sun et al., 2009).

It is noteworthy that these studies used human MSCs in murine models for human cancers and we wondered whether possible unphysiological, non-specific functions of human cells in a murine context could be the cause of the observed effects of MSCs on tumor cells. Therefore, we compared the homing potential of murine and human MSCs after systemic administration and their potential capacity for metastasis induction in various cancer models.

Results

Tissue distribution of murine and human MSCs

MSCs derived from bone marrow have the potential to differentiate in vitro along numerous mesenchymal lineages (Mackay et al., 1998; Wakitani et al., 1994; Majumdar et al., 1998). Only the induction of differentiation in vitro provides a test system to validate a specific MSC preparation for its pluripotency. We carried out differentiation to adipocytes, osteoblasts and chondrocytes on our murine (Supplementary Fig. 1A) and human MSCs (Supplementary Fig. 1B). After having established the stemness of our murine and human MSCs we went on to examine their tissue distribution following systemic administration and their potential to promote metastasis.

In order to test the tissue tropism of MSCs, we intravenously injected 1×10^5 CM-Dil labeled mouse and human MSCs, respectively, into nu/nu mice. One week post-injections we analyzed micro-sections from bone marrow, liver, lymph nodes, lung and spleen for the presence of MSCs (Fig. 1A, Supplementary Figs. 2A, B and for larger images of the magnified areas Supplementary Figs. 7A, B). Our quantitative analysis on sections of these tissues showed that more than 43–44% of both murine and human MSCs had infiltrated lymph nodes, 36% the spleen and 8–12% bone marrow and liver, whereas only 1–3% were detected in the lungs (Fig. 1B). Other tissues such as brain, heart, and kidney were virtually free of MSCs (data not shown). This means that there was no overall difference in the relative biodistribution pattern between murine and human MSCs. In order to provide the cell numbers, on which the relative biodistribution analysis (Fig. 1B) is based, we show the same profile using numbers of total detected MSCs in the five tissues (Fig. 1C). Furthermore, we analyzed the number of MSCs in relation to the total number of cells on sections from each of the tissues revealing that the density of MSCs is highest in liver, lymph nodes and spleen (Fig. 1D). These findings demonstrate that systemically injected MSCs from the two species behave similarly in a nu/nu mouse model.

Previous studies that had used different methods to detect MSCs (bioluminescent imaging and real-time PCR, respectively) and had analyzed MSC bio-distribution over a wider time course including very short-time points following the administration of MSCs (Kidd et al., 2009; Lee et al., 2009) had shown a pronounced accumulation of MSCs in the lungs on day 1 that started to disappear 5 days after the injection of MSCs. At this time point the cells started to be detectable in liver and spleen in increasing numbers, similar to our results. In order to validate our results and render them comparable to the before mentioned studies we conducted an experiment including a short time point. To this end, we examined the numbers of Dil-labeled human MSCs in the lung 15 min after injection and compared it to the values after 1 week (Supplementary Figs. 3A, B, C). We found a 6.5-fold reduction of the MSC numbers in the lungs over this time frame, which is broadly in line with the previous reports.

Tissue distribution of murine MSCs in syngenic, immune-competent mice

In order to evaluate the tissue distribution of MSCs in a fully syngenic model, we used murine FVB-derived MSCs in FVB/N mice. We intravenously injected 1×10^5 CM-Dil labeled mouse MSCs and analyzed bone marrow, liver, lymph nodes, lung and spleen for the presence of MSCs 1 week after the injections (Fig. 2A and for larger images of the magnified areas Supplementary Fig. 8). The quantitative analysis showed a three fold drop in detected MSCs as compared to immune-deficient mice, but an almost equivalent presence of MSCs in bone marrow, liver and lymph nodes, with 25% of all detected MSCs in each of the three tissues. The remaining cells were found with 9% in the lungs and 17% in the spleen (Figs. 2B, C). In comparison to nu/nu mice we found relatively small differences in the tissue distribution pattern of MSCs in this syngenic model. The most striking differences were that relatively more cells homed to the bone marrow and the liver. This led to a higher cellular density of MSCs in the liver and fewer MSCs in lymph nodes and spleen in relation to the total number of cells on the analyzed tissue sections (Fig. 2D). However, the overall trend of infiltration of substantial numbers of MSCs in lymphatic tissue, liver, spleen and bone marrow on the one side and substantial smaller numbers in the lungs at this time point remained the same. These findings demonstrate that the bio-distribution of systemically injected MSCs is broadly similar in immune-deficient and immune-competent mice.

Tissue distribution of MSCs over time and in tumor-burdened animals

Next, we investigated whether the tissue distribution of MSCs might change over time and whether differences between murine and human cells might become apparent at this later time point post-injection. Our results show that after 4 weeks the relative tissue distribution pattern of the MSCs was overall unchanged (Fig. 3A) as compared to the one-week time point. Again, MSCs did not appear in the other organs (brain, heart, kidney) in any substantial numbers (data not shown).

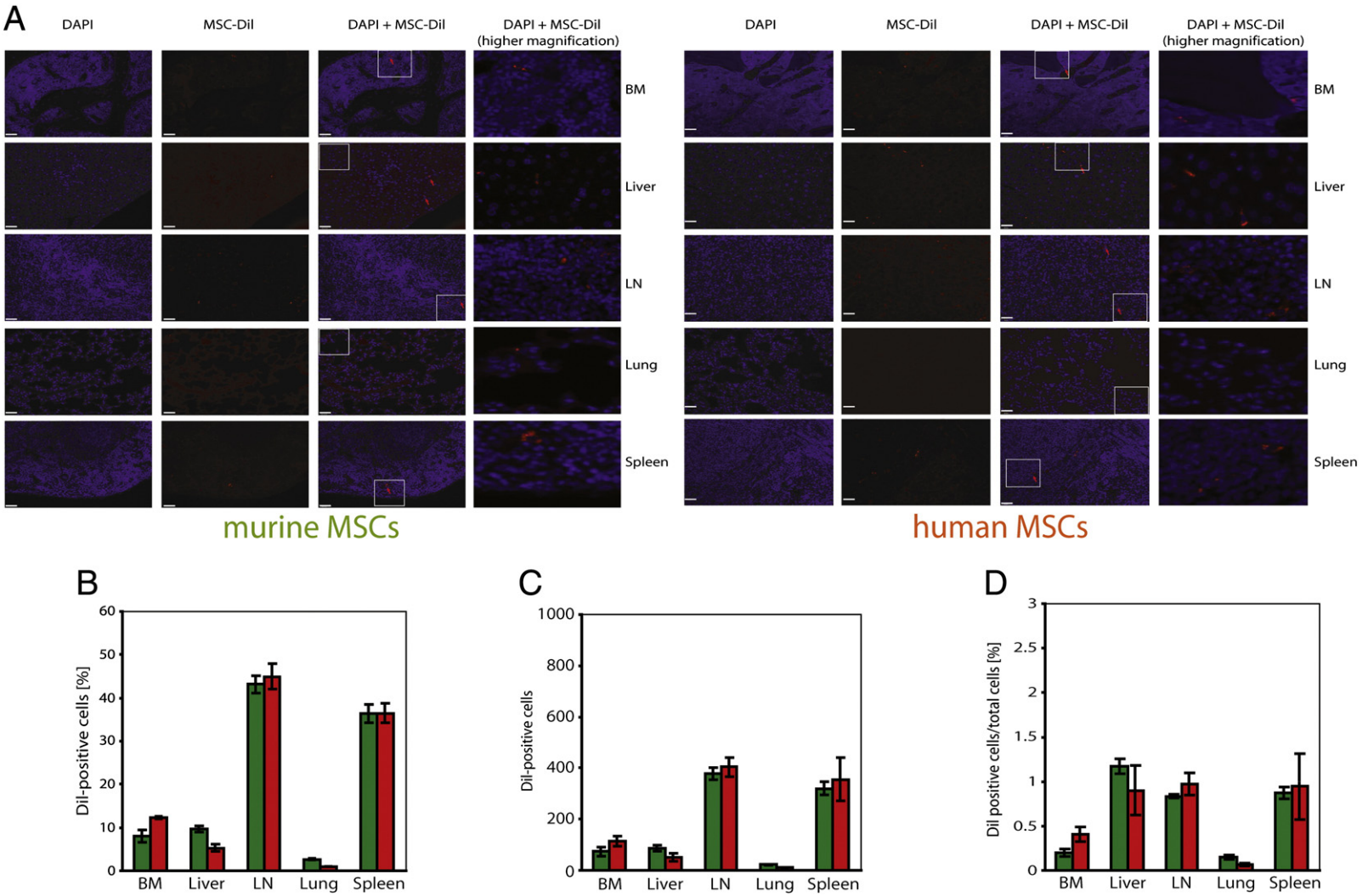

Figure 1 Tissue distribution of murine and human MSCs. (A): CM-Dil labeled murine (left panels) and human MSCs (right panels) are present in bone marrow (BM), liver, lymph nodes (LN), lung and spleen. The MSCs are indicated by red arrows. The tissues were counterstained with DAPI. The DAPI stains are depicted in the first column of images, the CM-Dil label in the second column, the superimposed images of DAPI and CM-Dil in the third column and images of magnified areas, which are indicated by a white-lined box, in the fourth column. Shown are representative images. (B): Quantification of the relative tissue distribution of murine (green bars) and human (red bars) MSCs 1 week after intravenous injection. (C): Quantification of the total number of murine (green bars) and human (red bars) MSCs in the analyzed microsections from the respective tissues 1 week after intravenous injection. (D): Depicted are the number of murine (green bars) and human (red bars) MSCs in relation to the total number of cells in the analyzed sections. For the analyses, a total of 15 randomly chosen fields were counted for each tissue. Four animals per group were analyzed.

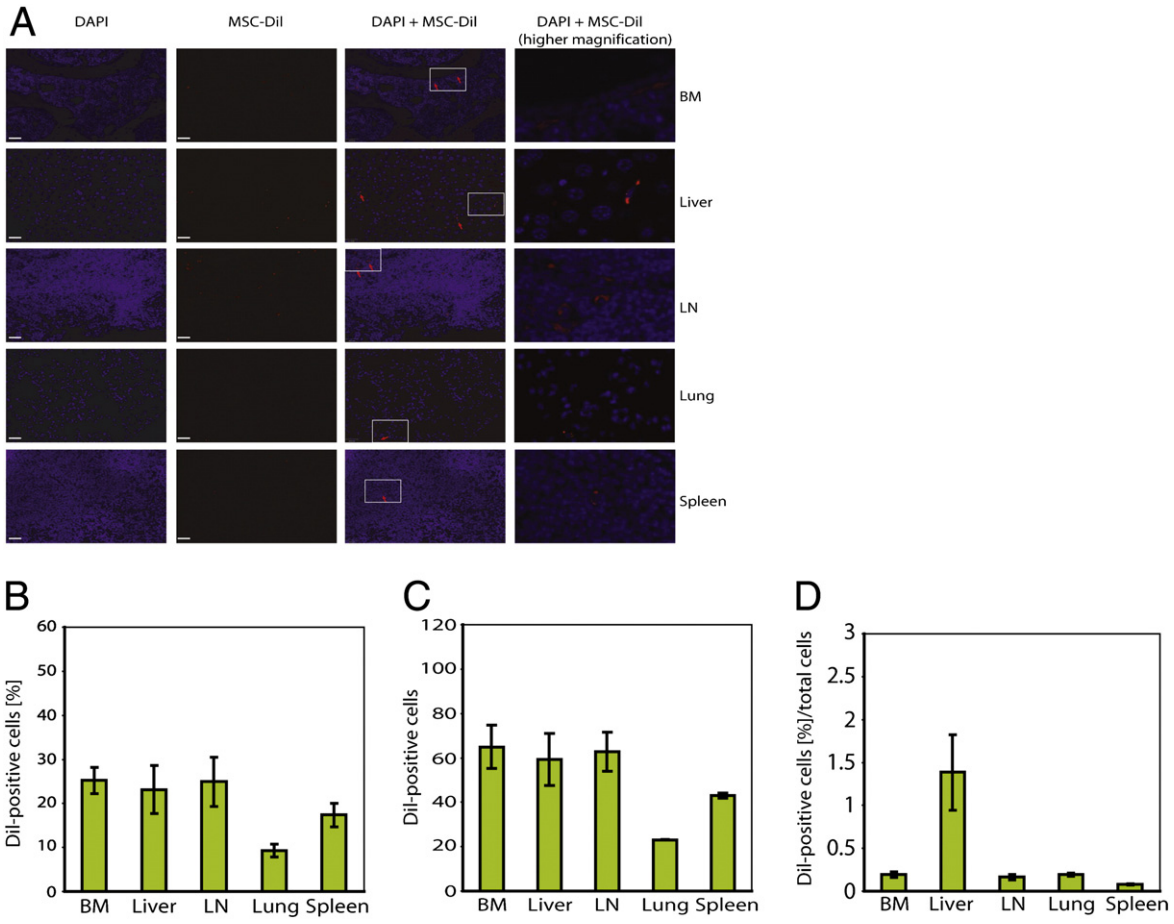

Figure 2 Bio-distribution of murine MSCs (derived from FVB/N mice) in immune-competent FVB/N mice. (A): CM-Dil labeled murine MSCs are present in bone marrow (BM), liver, lymph nodes (LN), lung and spleen. The MSCs are indicated by red arrows. The tissues were counterstained with DAPI. The DAPI stains are depicted in the first column of images, the CM-Dil label in the second column, the superimposed images of DAPI and CM-Dil in the third column and images of magnified areas, which are indicated by a white-lined box, in the fourth column. Shown are representative images. (B): Quantification of the relative tissue distribution of murine MSCs 1 week after intravenous injection. (C): Quantification of the total number of murine MSCs in the analyzed microsections from the respective tissues 1 week after intravenous injection. (D): Depicted are the numbers of murine MSCs in relation of the total number of cells in the analyzed sections. For the analyses, a total of 15 randomly chosen fields were counted for each tissue. Three animals were analyzed.

Regarding the cell numbers, on which the relative bio-distribution analysis (Fig. 3A) is based, we show that the profile was not markedly altered when using numbers of total detected MSCs in the five tissues in comparison to the results of one week post-injections (Fig. 3B). Similarly, the cellular density of MSCs in the different tissues was also broadly unchanged (Fig. 3C). We then hypothesized that the presence of tumor cells might influence the behavior of MSCs and that a species specific difference might become apparent then. However, when we had established MDA-MB-231 human breast cancer xenografts in nu/nu mice before we injected 1×10^5 CM-Dil labeled MSCs we observed no substantial differences in the tissue distribution profile of murine and human MSCs in tumor-burdened animals (Figs. 3D, E). We did, however, notice, a rise in the number of MSCs in tumor-burdened animals (Fig. 3E) also resulting in a higher proportion of MSCs in relation to the total number of cells in the analyzed organs (Fig. 3F). Interestingly, the tumor-induced increase in MSC numbers was more pronounced with murine MSCs as compared to human MSCs. Hence, significantly more murine MSCs than human MSCs were found in the tumor burdened animals, in particular in spleen, lymph nodes and lungs, as murine MSCs either proliferated more profoundly, were better protected from cell death or were retained more effectively in the tissues. In a subsequent, separate experiment we included the primary xenografts in our analyses and showed that a proportion of the injected MSCs had homed to the tumors (Supplementary Fig. 4A). Quantification of the bio-distribution of murine and human MSCs in this experiment showed that between 2%–5% of the cells were found in the tumor masses (Supplementary Fig. 4B). The numbers of MSCs in tumor tissue sections were relatively low (Supplementary Fig. 4C) but contributed to cellular density of the tumor almost to the same degree as in bone marrow and lymph nodes (Supplementary Fig. 4D). The distribution pattern in the other tissues was comparable to the results shown in Figs. 3D–F with the values only reduced by the small fraction of the tumor-infiltrating MSCs (Supplementary Figs. 4B, C, D). Again, we found significantly more murine MSCs than human MSCs in particular in

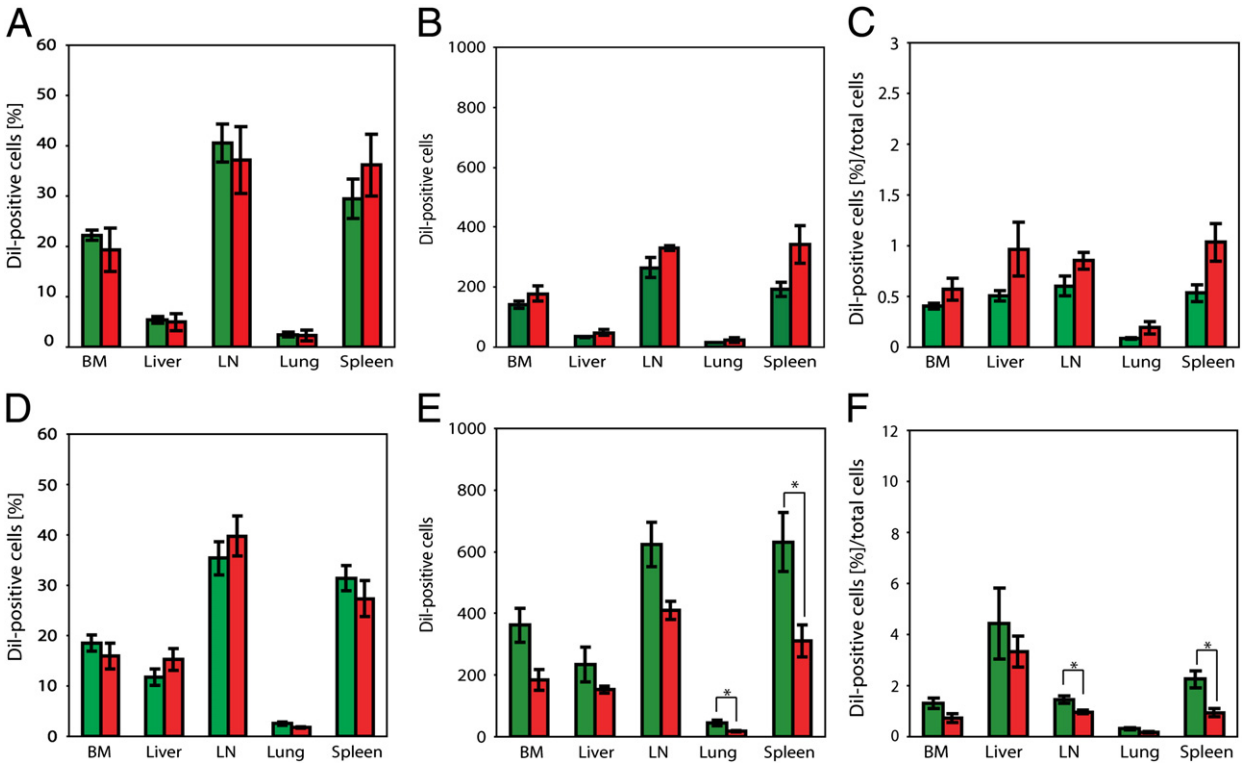

Figure 3 The tissue distribution profile of MSCs does not change over time and in tumor burdened animals. (A): Quantification of the relative distribution of murine (green bars) and human (red bars) MSCs 4 weeks after intravenous injection. (B): Quantification of the total number of murine (green bars) and human (red bars) MSCs in the analyzed microsections from the respective tissues 4 weeks after intravenous injection. (C): Depicted are the number of murine (green bars) and human (red bars) MSCs in relation to the total number of cells in the analyzed sections 4 weeks after intravenous injection. (D): Quantification of the relative distribution of murine (green bars) and human (red bars) MSCs 4 weeks after intravenous injection into tumor burdened animals. (E): Quantification of the total number of murine (green bars) and human (red bars) MSCs in the analyzed microsections from the respective tissues 4 weeks after intravenous injection into tumor burdened animals. (F): Depicted are the number of murine (green bars) and human (red bars) MSCs in relation to the total number of cells in the analyzed sections of tumor-burdened animals. For the analyses, a total of 15 randomly chosen fields were counted for each tissue. For the non-tumor burdened analyses three animals per group and for the tumor-burdened analyses seven animals per group were analyzed.

the spleen and lungs, but also in bone marrow and lymph nodes. There was no significant difference between murine MSCs and human MSCs in the primary tumor tissue. These findings demonstrate that the established tumors did impact on the total numbers of MSCs, but did not affect the general tropism of both, murine and human MSCs, and their bio-distribution profile.

Both human and murine MSCs promote metastasis

Finally, we examined the impact of MSCs on metastatic behavior of cancer cells. First, we used MDA-MB-231 human breast cancer cells. After having established MDA-MB-231 human breast cancer xenografts in nu/nu mice for 3 weeks, we injected 1×10^5 CM-Dil labeled murine or human MSCs into the tail vein. Four weeks after the injection of MSCs we examined bone marrow, liver, lymphnodes, lung and spleen from these animals for metastasis formation on H&E stained sections of these tissues (Fig. 4A). We found that 54% and 42% of all animals that were treated with murine and human MSCs, respectively, had metastatic growths in their lungs and in some rare cases in the liver (Fig. 4B). In control animals that were not injected with MSCs we could detect metastatic nodules in the lung in only 17% of the mice and none in the liver (Fig. 4B). Furthermore, in animals that received murine or human MSCs but no tumor cells we could not detect lesions in lungs or liver ruling out that MSCs form neoplastic nodules in our experimental model (Fig. 4B).

When we compared the extent of metastatic growth in animals that received murine MSCs to those that received cells of human origin, we found that the former exhibited more aggressively growing tumor nodules in the lung (Fig. 4C). In order to confirm that the lesions did indeed originate from human MDA-MB-231 mammary carcinoma cells we stained lung microsections from tumor-burdened mice that were injected with murine MSCs with an antibody specific to human CD326. The antibody detected human CD326 on the surface of cells in tumor nodules in the lung (Supplementary Fig. 5A), whereas lungs from non-tumor burdened animals that had been injected with murine MSCs exhibited no lesions in their lungs (Supplementary Fig. 5B) and were negative for human CD326 (Supplementary Fig. 5C). Furthermore, in an immuno-cytochemical study the CD326 antibody only emits a signal

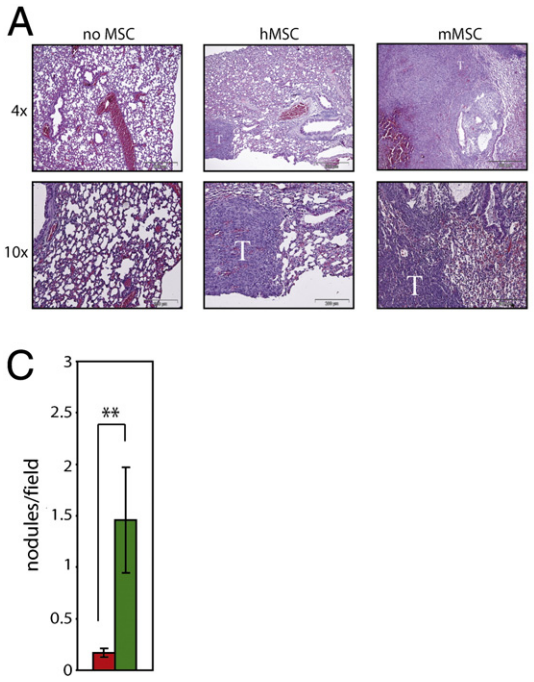

B

	animals with lung metastasis	animals with lung metastasis [%]
MDA/ no MSCs	1 (6)	17
MDA/ human MSCs	5 (12)	42
MDA/ murine MSCs	7 (13)	54

	animals with liver metastasis	animals with liver metastasis [%]
MDA/ no MSCs	0 (6)	0
MDA/ human MSCs	1 (12)	8
MDA/ murine MSCs	1 (13)	8

	animals with lung metastasis	animals with lung metastasis [%]
no MDA human MSCs	0 (6)	0
no MDA murine MSCs	0 (11)	0

Figure 4 Both human and murine MSCs can promote metastasis (A): Analysis of lung metastasis in MDA-MB-231 tumor-burdened animals that received no MSCs (left), human MSCs (hMSC; center) or murine MSC (mMSC; right). Tumor tissue is marked by a white T. Shown are representative images of H&E stained microsections of lung tissues. The images show that both human and murine MSCs promote metastasis but the latter give rise to more aggressively growing tumor nodules. (B): Quantification of the occurrence of lung (upper table) and liver (middle table) metastatic lesions in MDA-MB-231 tumor-burdened mice that received no MSCs, human MSCs or murine MSC as well as control mice (lower table) that only received murine MSCs and human MSCs, respectively. Shown are the number of animals with metastasis and the total number of animals analyzed from each group (number in parenthesis) as well as the percentages of affected animals. (C): Quantification of the number of metastatic nodules in MDA-MB-231 tumor-burdened mice that received human MSCs (red bar) or murine MSC (green bar) demonstrating that murine MSCs possess a higher pro-metastatic activity than human MSCs in our model system. For these analyses, 20 randomly chosen low-power fields from human lung sections and 24 murine lung sections were counted.

when incubated with MDA-MB-231 cells but not with human and mouse MSCs further demonstrating the specificity of the antibody (Supplementary Fig. 5D). Moreover, when we examined lung tumor lesions from tumor-burdened mice that were injected with CM-DiI labeled murine MSCs we could detect single MSCs inside as well as outside of the lesions, but in no case was the nodule made up entirely or in its majority from red-fluorescing MSCs (Supplementary Fig. 5E). Hence, while we cannot completely rule out that (transformed) MSCs also form metastasis-like nodules, our results show that the lesions we detected, at least in the majority, stemmed from human breast cancer cells. These findings demonstrate that murine as well as human MSCs can promote metastasis formation of mammary carcinoma cells.

In addition, we tested the metastasis-promoting potency of MSCs in two additional tumor models, the 4T1 breast cancer and the HCT116 colorectal cancer model. 4T1 cells are highly metastatic, murine breast cancer cells and have been extensively used to study the tumor dissemination process. We subcutaneously injected 5×10^6 of 4T1 cells into the flank of BALB/c mice and waited until the primary tumor was palpable, usually after 1 week. Then, we intravenously injected 1×10^5 MSCs into the tumor-burdened mice. After 3 weeks we examined the lungs of these animals for metastases and found that all mice regardless of whether they had received MSCs or not had developed cancerous growth in their lungs (Supplementary Figs. 6A, B). Quantification of the metastatic burden, both on a macroscopic and microscopic level, also revealed no significant differences between the cohorts (Supplementary Fig. 6C). Hence, 4T1 cells possess metastatic properties that cannot be further enhanced by the action of MSCs. Therefore, we turned to a third tumor cell type, namely HCT116 cells that normally do not disseminate when grown as subcutaneous xenografts. In this model no lung metastases formed in control animals (no MSCs), but in animals injected with MSCs we found metastatic lesions in 3 out of 5 mice (Supplementary Figs. 6D, E, F). In summary, MSCs exert pro-metastatic effects on low to medium invasive tumor cells, but seem to fail to further aggravate the metastatic potential of highly aggressive cancers.

Discussion

MSCs have been proposed as cellular tumor therapy vehicle, either utilizing their proposed intrinsic anti-cancer properties or in combination with the expression of therapeutic transgenes. Furthermore, MSCs have been used and even tested in clinical trials for a variety of degenerative disorders and as immune-suppressors in for example Graft-versus-host

disease (GvHD). Thus, while the potential beneficial utility of MSCs appears plentiful (Motaln et al., 2010; Baksh et al., 2004), Karnoub et al. (Karnoub et al., 2007) have reported that human MSCs promote the development of metastasis in a human breast cancer model. These results raise serious concerns regarding the safe use of MSCs in cell therapeutic applications in general and tumor treatments in particular. We asked whether the use of human MSCs in those studies might have led to unspecific effects owing to a non-physiological tropism of the human cells in a mouse organism. Therefore, we examined and quantified the locations of systemically administered human MSCs and compared them to their murine counterparts. We found no difference with regard to the total number of cells as well as relative tissue distribution between MSCs from the two species, which also did not change over time. Furthermore, we asked whether the presence of a tumor could influence the homing characteristics of MSCs. While we detected an overall increase in the numbers of MSCs, in particular of murine MSCs, in tumor-burdened animals, we found no differences between murine and human MSCs in the overall tissue distribution profile as well as no changes compared to non-tumor burdened animals. Hence, it appeared unlikely that the metastasis promoting activity of human MSC was caused by an unusual tissue distribution. Finally, we examined the impact of systemically administered MSCs on the capacity of human mammary carcinoma cells to metastasize and found that both murine and human cells promoted the formation of metastatic lesions in the lungs. Further analysis revealed that murine MSCs caused more highly aggressive lesions compared to human MSCs. These findings argue for an evolutionary conserved signal or signals that mediate the pro-metastatic activity of MSCs and highlight the feasibility of transgenic murine model systems to study the role of MSCs in metastasis development, thereby providing a potential valuable research tool for elucidation of the cellular and molecular mechanisms during tumor dissemination. When we used two other human cancer models, a highly metastatic mammary cancer cell line, 4T1, and a non-metastatic human colorectal cancer cell line, HCT116, we found that MSCs did not significantly promote dissemination of 4T1 tumors, whereas metastasis development was dramatically increased in the HCT116 model. These results indicate that highly malignant cancer cells possess sufficient intrinsic metastatic potential that cannot be further enhanced by signals emitted by MSCs, whereas tumor cells with little metastatic activity appear to receive cues from MSCs that increase their dissemination to distal organs. The chemokine CCL5 (also known as RANTES) secreted from MSCs and its cognate receptor CCR5 expressed on the surface of cancer cells have been implicated in this process (Karnoub et al., 2007). However, while the CCL5-CCR5 axis appeared to be responsible for the pro-metastatic function of MSCs in MDA-MB-231 and MDA-MB-435 breast carcinoma cells, it had no effect in a number of other mammary cancer cells, pointing to the existence of additional or alternative signals.

Moreover, we cannot completely rule out that MSCs in the lungs, where they home to in large numbers immediately after injection, create a pre-metastatic niche for tumor metastasis to develop later. However, the findings by Karnoub et al.(2007) and the time gap between MSC-infiltration and appearance of metastatic lesions in the lungs make this explanation less likely. Irrespective of the two possible mechanisms, i.e. interaction between mesenchymal cells and tumor cells vs. creation of a pre-metastatic niche, the analysis and elucidation of the underlying molecular factors and pathways might provide new ways to prevent and/or treat metastatic disease.

For MSCs as a cellular therapeutic it means that the factors that afford their pro-metastatic activity have to be fully identified and then eliminated so that they can be used safely.

Material and methods

Reagents

All chemicals, reagents and media, unless otherwise stated, were purchased from Sigma. TGF-β was purchased from Peprotech.

Cell culture

The breast cancer cell line MDA-MB-231 was cultured in DMEM medium (Invitrogen) supplemented with 10% fetal bovine serum (FBS) (Invitrogen), 100 U/ml Penicillin, 100 μg/ml Streptomycin and 1% L-glutamine. Murine mammary carcinoma 4T1 cells were cultured in RPMI-1640 medium (Invitrogen) supplemented with 10% FBS, 100 IU/ml Penicillin, 100 μg/ml Streptomycin and 1% L-glutamine. Human colorectal cancer HCT116 cells were cultured in McCoy's medium (Lonza) supplemented with 10% FBS, 100 U/ml Penicillin, 100 μg/ml Streptomycin and 1% L-glutamine.

Human MSCs were from Lonza and cultured in low glucose DMEM, 10% FBS and 100 U/ml penicillin and 100 μg/ml streptomycin.

Isolation and expansion of murine MSCs

Inbred FVB/N mice, 4–6 weeks old, were sacrificed using CO_2 and their tibias and femurs were dissected and cleaned of all soft tissue. The epiphysis of each bone was clipped, and the bone marrow was flushed out by inserting a syringe needle (20-gauge) into the end of the bone, and suspended in cold DMEM-low glucose containing 100 U/ml penicillin and 100 μg/ml streptomycin. After centrifugation the cells were resuspended and plated in T-75 tissue culture flasks using DMEM-low glucose containing 100 U/ml penicillin and 100 μg/ml streptomycin and 15% FBS (Invitrogen). Flasks were kept in a humidified incubator in an atmosphere of 5% CO_2 at 37 °C. The first medium replacement was done on day 3, and subsequent changes of the medium were performed every 4 days. About 7–9 days after culture initiation, several clones of fibroblast-shaped cells emerged. When they reached 80–90% confluence, cultures were washed with warm PBS, and incubated at 37 °C in pre-warmed 0.25% trypsin and 0.53 mM EDTA for 2 min. Based on the method of Peister et al. (Peister et al., 2004) for murine MSC isolation, only detached cells after 2 min trypsin incubation were pooled and cultured in T-75 flasks as passage-1 cells. The cells were subsequently expanded in DMEM-low glucose with 100 U/ml penicillin and 100 μg/ml streptomycin and 15% FBS. We used cells from passages 3–5 for our experiments.

Differentiation assays of human and murine MSCs

For osteogenic differentiation early-passage cells were plated at 2×10^5 cells/well in a 6-well plate and incubated in DMEM-low glucose supplemented with 15% FBS until confluence was achieved. The medium was then replaced with an osteogenic induction medium (Iscoves supplemented with 50 μM ascorbic acid 2-phosphate, 100 nM dexamethasone and 20 mM β-glycerol phosphate, 50 ng/ml L-thyroxine, 9% FBS, 9% equine serum, 2 mM L-glutamine 100 U/ml penicillin and 100 μg/ml streptomycin). In addition, some plates were incubated with complete medium (Iscoves, 9% FBS, 9% equine serum, 2 mM L-glutamine 100 U/ml penicillin and 100 μg/ml streptomycin) to be used as controls. Medium was changed every 2 days over a total of 21 days. Cells were then fixed with 10% formalin for 10 min and Von-Kossa staining was carried out as follows: after being rinsed with water, cells were covered with 3% silver nitrate solution for 10 min in the absence of light. Cells were then rinsed and the plate was exposed to bright warm light for 15 min. After rinsing with water images were taken.

Chondrogenesis differentiation was performed by pelleting approximately 200,000 cells by centrifugation at 300×*g* for 4 min, followed by incubation at 37 °C in 5% CO_2 in 1 ml chondrogenic medium, composed of DMEM-high glucose, 1% FBS, 50 μg/ml ascorbic acid 2-phosphate, 100 nM dexametasone, 40 μg/ml L-proline, 1 mM sodium pyruvate, 10 ng/ml TGF-β, 100 ng/ml BMP-2, ITS+supplement (final concentration: 6.25 μg/ml bovine insulin, 6.25 μg/ml transferrin, 6.25 μg/ml selenous acid, 5.33 μg/ml linoleic acid, 1.25 mg/ml BSA) and 100 U/ml penicillin and 100 μg/ml streptomycin. After 24 h cells begun to contract and to form a disk-like structure. Medium was changed three times a week by aspirating off as much medium as possible without disrupting the pellet and replacing it with 0.5 ml of fresh chondrogenic medium. After 21 days in culture the pellets were harvested by aspirating off all medium and washing twice in PBS. Pellets were then fixed for 1 h in 10% formalin at room temperature, and paraffin embedded. Toluidine blue staining was carried out by incubation of deparaffinized and rehydrated sections of pellets in 0.5% toluidine blue solution (pH 2.5) at room temperature. Slides where then washed in deionized water, dehydrated and mounted.

For adipogenesis, cells were plated at 2×10^5 cells/well, in a 6-well plate and incubated in DMEM-low glucose supplemented with 15% FBS until full confluence was achieved. Then medium was replaced with differentiation medium consisting of DMEM-high glucose, supplemented with 15% FBS, 1 mM dexamethasone, 1 mg/ml insulin, 100 mM indomethacin, 500 mM MIX (3-isobutyl-1-methyl-xanthine), 100 U/ml penicillin and 100 μg/ml streptomycin. Cells were incubated at 37 °C and 5% CO_2 for 72 h. Control cells received normal growth medium. After 72 h, the medium on differentiation-induced cells was replaced with maintenance medium consisting of DMEM-high glucose, supplemented with 15% FBS, 100 U/ml penicillin and 100 μg/ml streptomycin and the cells grown for another 2 days. Three cycles of induction and maintenance media changes were completed before cells were left in maintenance medium for a total of 5–7 days. At the end of this period, the cells were fixed for 10 min in 10% formalin and stained with 0.5% Oil Red O solution. After a 5 min incubation step at room temperature, excess dye solution was removed by washing with 60% isopropanol, and counterstaining was carried out with Harris-Hematoxylin 1:5 solution in water.

CM-Dil labelling of MSCs

MSCs were loaded with 4 μg/ml Chloromethyl-dialkyl-carbocyanine (CM-Dil) (Invitrogen) in pre-warmed PBS for 15 min at 37 °C followed by an incubation for 15 min at 4 °C. The cells were washed with PBS, resuspended in their normal growth medium and cultured for 16 h before they were used.

Immuno-fluorescence studies

Four μm-paraffin tissue sections were deparaffinized and rehydrated. Then samples were washed in PBS and antigen unmasking was carried out in 0.01 M citric acid pH 6 using a microwave for 10 min. Samples were cooled down to room temperature, washed and blocked for 1 h at room temperature. After the mouse anti-human CD326 (Novus Biologicals) incubation at 4 °C overnight, the sections were washed and the fluorophore sheep anti-mouse Dylight 488 (Jackson Immunoresearch) was used as secondary antibody. After the secondary antibody incubation, slides were washed in PBS, incubated for 10 min in DAPI and mounted in fluoromount solution.

For quantification of MSC bio-distribution, 4 μm paraffin sections were deparaffinized and rehydrated, washed in PBS, followed by an incubation for 10 min with DAPI, and mounted in fluoromount solution for the detection of fluorescent cells under a microscope. 15 randomly chosen fields/organ of each animal were counted.

Animal studies

Ten week old female CD1 nu/nu mice (Charles River) were subcutaneously injected with 5×10^6 tumor cells (MDA-MB-231 or HCT116) in 200 μl PBS under the lateral skin of the right leg. Ten week old female BALB/c mice (Charles River) were subcutaneously injected with 5×10^6 4T1 tumor cells in 200 μl PBS under the lateral skin of the right leg. When tumors were palpable, the animals were injected intravenously with 1×10^5 CM-Dil labeled MSCs.

For the analysis of the tissue distribution of the MSCs and their effects on metastasis formation inguinal, axillary, mesentheric and paraaortic lymph nodes, liver, spleen, kidney, and lung were fixed in 10% formalin. In addition, tibia and femur, and vertebra of each animal were formalin fixed, followed by decalcification with a solution of 8% formic acid/8% HCl prior to tissue processing and paraffin embedding.

The animal studies were performed according to national laws and covered by license from the Irish government.

Histopathology

Organ specimens were fixed in 10% neutral buffered formalin, and 4 μm-paraffin sections were stained with hematoxylin and eosin (H&E) and examined using light microscopy.

Statistical and quantitative analyses

Experimental values are always expressed as mean value ± standard error. For significance analysis ANOVA was used. The exact p-values for the bio-distribution analyses are provided in the supplementary material section (Supplementary Tables). We considered $p<0.05$ as significant (*) and $p<0.01$ as highly significant (**).

First, we counted the number of Dil-labeled MSCs in bone marrow, spleen, liver, lymph nodes, and tumor and expressed the numbers found in each of the tissues as percentage of the total Dil-labeled MSCs that we counted. Hence, the figures express the relative distribution of MSCs in these tissues. Additionally, we have counted the total number of non-labeled cells in the sections and expressed the number of MSCs as percentage of total cells. This provides a measure for the cellular density of MSCs in the respective organs.

Supplementary materials related to this article can be found online at doi:10.1016/j.scr.2011.05.002.

Acknowledgments

Ralf M. Zwacka is supported by an EU-FP6 Marie-Curie Excellence Team Award (MIST). The work was also supported by an EU-RTN Award (ApopTrain) and a Research Frontier Project Grant from Science Foundation Ireland (BIM084) (to R. M. Z).

We thank the staff of the Science Foundation Ireland funded Regenerative Medicine Institute (REMEDI) for their advice and support.

References

Baksh, D., Song, L., Tuan, R.S., 2004. Adult mesenchymal stem cells: characterization, differentiation, and application in cell and gene therapy. J. Cell Mol. Med. 8, 301–316.

Barry, F.P., Murphy, J.M., 2004. Mesenchymal stem cells: clinical applications and biological characterization. Int. J. Biochem. Cell Biol. 36, 568–584.

Dominici, M., Le Blanc, K., Mueller, I., Slaper-Cortenbach, I., Marini, F., Krause, D., Deans, R., Keating, A., Prockop, D., Horwitz, E., 2006. Minimal criteria for defining multipotent mesenchymal stromal cells. The International Society for Cellular Therapy position statement. Cytotherapy 8, 315–317.

Hall, B., Dembinski, J., Sasser, A.K., Studeny, M., Andreeff, M., Marini, F., 2007. Mesenchymal stem cells in cancer: tumor-associated fibroblasts and cell-based delivery vehicles. Int. J. Hematol. 86, 8–16.

Karnoub, A.E., Dash, A.B., Vo, A.P., Sullivan, A., Brooks, M.W., Bell, G.W., Richardson, A.L., Polyak, K., Tubo, R., Weinberg, R.A., 2007. Mesenchymal stem cells within tumour stroma promote breast cancer metastasis. Nature 449, 557–563.

Khakoo, A.Y., Pati, S., Anderson, S.A., Reid, W., Elshal, M.F., Rovira, I.I., Nguyen, A.T., Malide, D., Combs, C.A., Hall, G., et al., 2006. Human mesenchymal stem cells exert potent antitumorigenic effects in a model of Kaposi's sarcoma. J. Exp. Med. 203, 1235–1247.

Kidd, S., Spaeth, E., Dembinski, J.L., Dietrich, M., Watson, K., Klopp, A., Battula, V.L., Weil, M., Andreeff, M., Marini, F.C., 2009. Direct evidence of mesenchymal stem cell tropism for tumor and wounding microenvironments using in vivo bioluminescent imaging. Stem Cells 27, 2614–2623.

Lee, R.H., Pulin, A.A., Seo, M.J., Kota, D.J., Ylostalo, J., Larson, B.L., Semprun-Prieto, L., Delafontaine, P., Prockop, D.J., 2009. Intravenous hMSCs improve myocardial infarction in mice because cells embolized in lung are activated to secrete the anti-inflammatory protein TSG-6. Cell Stem Cell 5, 54–63.

Mackay, A.M., Beck, S.C., Murphy, J.M., Barry, F.P., Chichester, C.O., Pittenger, M.F., 1998. Chondrogenic differentiation of cultured human mesenchymal stem cells from marrow. Tissue Eng. 4, 415–428.

Majumdar, M.K., Thiede, M.A., Mosca, J.D., Moorman, M., Gerson, S.L., 1998. Phenotypic and functional comparison of cultures of marrow-derived mesenchymal stem cells (MSCs) and stromal cells. J. Cell. Physiol. 176, 57–66.

Mohr, A., Albarenque, S.M., Deedigan, L., Yu, R., Reidy, M., Fulda, S., Zwacka, R.M., 2010. Targeting of XIAP combined with systemic mesenchymal stem cell-mediated delivery of sTRAIL ligand inhibits metastatic growth of pancreatic carcinoma cells. Stem Cells 28, 2109–2120.

Molloy, A.P., Martin, F.T., Dwyer, R.M., Griffin, T.P., Murphy, M., Barry, F.P., O'Brien, T., Kerin, M.J., 2009. Mesenchymal stem cell secretion of chemokines during differentiation into osteoblasts, and their potential role in mediating interactions with breast cancer cells. Int. J. Cancer 124, 326–332.

Motaln, H., Schichor, C., Lah, T.T., 2010. Human mesenchymal stem cells and their use in cell-based therapies. Cancer 116, 2519–2530.

Peister, A., Mellad, J.A., Larson, B.L., Hall, B.M., Gibson, L.F., Prockop, D.J., 2004. Adult stem cells from bone marrow (MSCs) isolated from different strains of inbred mice vary in surface epitopes, rates of proliferation, and differentiation potential. Blood 103, 1662–1668.

Sleeman, J., Steeg, P.S., 2010. Cancer metastasis as a therapeutic target. Eur. J. Cancer 46, 1177–1180.

Son, B.R., Marquez-Curtis, L.A., Kucia, M., Wysoczynski, M., Turner, A.R., Ratajczak, J., Ratajczak, M.Z., Janowska-Wieczorek, A., 2006. Migration of bone marrow and cord blood mesenchymal stem cells in vitro is regulated by stromal-derived factor-1-CXCR4 and hepatocyte growth factor-c-met axes and involves matrix metalloproteinases. Stem Cells 24, 1254–1264.

Sporn, M.B., 1996. The war on cancer. Lancet 347, 1377–1381.

Studeny, M., Marini, F.C., Champlin, R.E., Zompetta, C., Fidler, I.J., Andreeff, M., 2002. Bone marrow-derived mesenchymal stem cells as vehicles for interferon-beta delivery into tumors. Cancer Res. 62, 3603–3608.

Sun, B., Roh, K.H., Park, J.R., Lee, S.R., Park, S.B., Jung, J.W., Kang, S.K., Lee, Y.S., Kang, K.S., 2009. Therapeutic potential of mesenchymal stromal cells in a mouse breast cancer metastasis model. Cytotherapy 11, 289–298.

Wakitani, S., Goto, T., Pineda, S.J., Young, R.G., Mansour, J.M., Caplan, A.I., Goldberg, V.M., 1994. Mesenchymal cell-based repair of large, full-thickness defects of articular cartilage. J. Bone Joint Surg. Am. 76, 579–592.

Zhang, Y., Daquinag, A., Traktuev, D.O., Amaya-Manzanares, F., Simmons, P.J., March, K.L., Pasqualini, R., Arap, W., Kolonin, M.G., 2009. White adipose tissue cells are recruited by experimental tumors and promote cancer progression in mouse models. Cancer Res. 69, 5259–5266.